



# COLLAPSE RESISTANCE ASSESSMENT OF BUCKLING-RESTRAINED BRACED STEEL FRAMES USING COMBINED DETERMINISTIC AND PROBABILITY ANALYSIS APPROACH

Mingming Jia<sup>1</sup>, Shan Gao<sup>2\*</sup>, Dagang Lu<sup>1</sup>, Feng Fu<sup>3</sup>, Hui Zhang<sup>1</sup>

<sup>1</sup> Key Lab of Structure Dynamic Behavior and Control of China Ministry of Education, Harbin Institute of Technology, Harbin, China

<sup>2</sup> Shaanxi Key Laboratory of safety and durability of concrete structures, Xijing University, Xi'an, China

<sup>3</sup> School of Mathematics, Computer Science and Engineering, City, University of London, London, UK

**SUMMARY:** *The load bearing capacity, global ductility and overall stability of steel frame can be improved significantly through the use of buckling-restrained braces (BRBs). Based on the open resource platform OpenSees, finite element models of two types of steel frame buildings, one is nine story steel frame (SF) building and another is buckling-restrained braced steel frames (BRBFs) buildings are developed. The structures were analyzed using both deterministic and probability analysis approach. No component-removal random incremental dynamic analysis (IDA) and component-removal random IDA are used to analyze collapse resistance of the buildings under seismic load. The collapse modes of SF and BRBFs under earthquakes are discovered. The nonlinear dynamic responses of SF and BRBFs are analyzed before and after the removal of certain critical components using the alternative path method (APM) approach stipulated by GSA and vertical IDA method respectively. Correspondently, the probabilistic fragility function of collapse likelihood of SF and BRBFs are also derived based on random vertical incremental dynamics analysis approach. The analytical results show that the use of buckling-restrained braces ensures alternative load path, therefore changes the failure modes and improve collapse resistance of structures.*

**KEYWORDS:** *eccentrically braced steel frame; collapse resisting capacity; failure modes; alternative path method; fragility*

## 1. INTRODUCTION

Buckling-restrained braced steel frames (BRBF) system is an effective seismic resisting system for buildings in need of ductile seismic design. The Buckling-restrained Braces (BRBs) would fail preceding the beams of columns, so that the main structure can be protected from the strong

---

Corresponding author: Shan Gao, Shaanxi Key Laboratory of safety and durability of concrete structures, Xijing University, Xi'an, China  
Email: [gaoshan@xijing.edu.cn](mailto:gaoshan@xijing.edu.cn)

earthquake ground motions effect and suffer less seismic damage. The careful design of BRBF provides for a system that can translate the inherent ductility of steel structural members into system ductility, thereby controlling the response of the structure under a severe earthquake and presenting an attractive alternative to conventional braced frames [1-2].

The failure modes and progressive collapse resisting capacity of structures have attracted more and more research attention. Kim et al. [3] investigated the collapse resisting capacity of steel moment resisting frames by using alternate path methods. Khandelwal et al. [4] conducted a numerical study whose results showed that special concentrically braced frames were less vulnerable to progressive collapse than traditional concentrically braced frames due to improved system and member layouts. Hariri-Ardebili et al. [5] compared the seismic collapse assessment of multistory steel concentrically braced frames with time history analyses (THA) and incremental dynamic analysis (IDA) methods. Kim et al. [6] investigated the load resisting capacity of the steel frames by vertical push-down analysis. The results showed that the load resistance of the steel frame increased as the number of stories and spans increased. Mahdavi-pour and Deylami [7] studied the seismic demands of low and mid-rise BRBFs and Dual-BRBFs by using the probabilistic seismic demand analysis (PSDA). The results showed that using of BRBFs as a dual system could reduce the residual drift demand and improve collapse resisting capacity significantly. Eletrabi and Marshall [8] conducted a research to prove the obvious impact of BRBs on the catenary action demands in steel framed structures. The results of the study highlighted the importance of incorporating BRBs in the future guidelines addressing the progressive collapse resistance of steel structures. Wongpakdee et al. [9] developed a new structural system, namely buckling-restrained knee braced truss moment frame. The new structure showed good load resisting capacity and low probability for collapse under the ground motions. Freddi et al. [10] used local engineering demand parameters to evaluate the seismic risk of coupled systems consisting of low-ductility RC frames and dissipative braces. Dyanati et. al [11] performed a comparative study of seismic performance of self-centering concentrically braced frame (SCCBF) systems with that of conventional CBF systems. Engineering demand hazard curves were generated using the developed probabilistic demand models. Güneyisi [12] conducted a seismic fragility and risk analysis whose results indicated that BRBs significantly improved the seismic behavior of the original building by increasing the median values of the structural fragility curves. Zanini et al. [13] highlighted how the process of record selection can significantly influence the final results, being a source of relevant uncertainty and presented a case study application. Costanzo et al. [14] summarized the EC8- compliant design procedure and compared the EC8 detailing rules with those recommended in US Code. Ferraioli et al. [15] stated that in the cases where the hardening behavior of the catenary action was fully developed, the analytical curve of DIF first decreased and

then increased with ductility.

For the study of BRB structure system, previous research studies are mainly focused on the seismic performance of BRBF. Most of them are deterministic research; the collapse resisting capacity of BRBF based on probabilistic analysis is rarely involved [16-17]. In this paper, random horizontal and vertical IDA are adopted to conduct the collapse resisting capacity assessment and derivation of collapse fragility of steel frames and BRBFs. The functions of BRBs and the failure modes of pertinent structures are identified based on the collapse analysis.

## **2. FINITE ELEMENT MODEL**

### *2.1 Prototype structure*

A 9-story structure designed for the Seismic Analysis Code (SAC) Phase III Steel Project is used for this study, which represents a typical mid-rise building designed in Los Angeles, California region. This building serves as a benchmark structure for SAC studies. The building's lateral stability system consists of steel perimeter moment-resisting frames (MRFs) and BRBs.

As shown in Fig. 1 (a), the nine-story structure is 45.75m by 45.75 m in plan, and 37.17 m in height. The stability system is one of the typical N-S MRFs used in California region. The floor-to-floor height for the first floor is 5.49m and 3.96 m for other floors. The lateral load-resisting systems of the structure are steel moment-resisting frames (MRF) and two different arrangements of BRBs. The MRF structure is laterally restrained at 1st level as shown in Fig. 1 (b). The MRF installed with BRBs and two arrangements of BRBs are depicted as shown in Fig. 1 (c)-(d). It should be mentioned that same columns are used in both steel moment-resisting frames and the frames with BRBs, in order to assess the effect of BRBs on providing alternative load path and redistribute internal force to prevent structural collapse explicitly.

The floor system is composite floor slab using wide-flange beams. The inertial forces caused by seismic load on each level are assumed to be carried uniformly by the floor diaphragm and transmitted to perimeter MRF, hence each MRF frame resists one sixth of the mass source of the entire structure. The mass and sizes of structural members of the model are listed in Table 1. The total stiffness of BRBs for each story is 6 times of the stiffness of that provided from the MRF. The detailed parameters of the model are listed in Table 1.

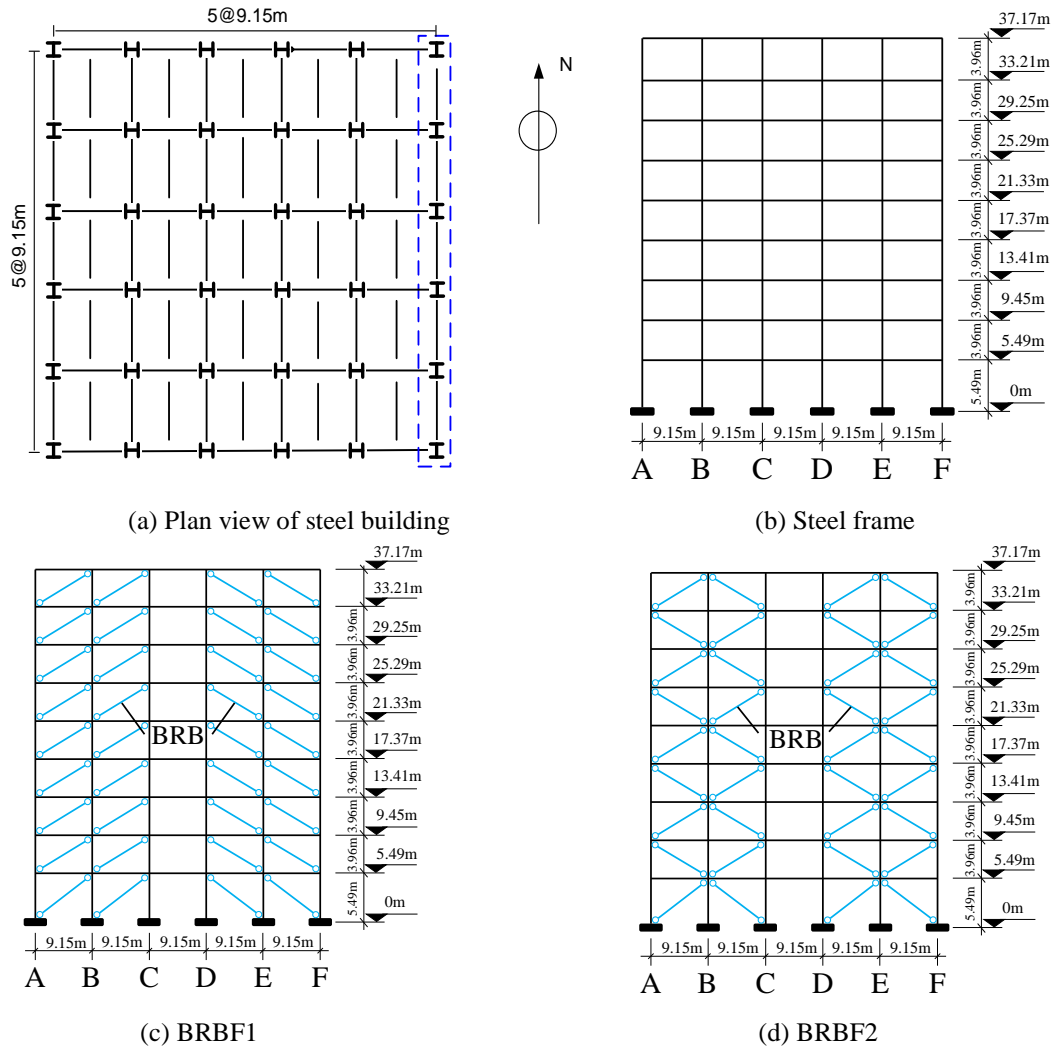


Figure 1 9-story buckling-restrained braced steel frames

Table 1 Parameters of the model

Floor	1st	2nd	3rd	4th	5th	6th	7th	8th	9th
Seismic mass/t	1010	989	989	989	989	989	989	989	1070
Cross sections of beam	W36×160W36×160W36×135W36×135W36×135W36×135W30×99 W27×84 W24×68								
Cross sections of column	W14×500W14×500W14×455W14×455W14×370W14×370W14×283W14×283W14×257								
Total cross section areas of BRBs/cm <sup>2</sup>	123.0	95.7	82.8	75.1	70.9	69.1	60.1	48.4	32.3

2.2 Modeling technique

The BRBs are modeled by truss element in open source software platform OpenSees, whilst columns and beams are modeled by “nonlinearBeamColumn” element. The A36, A588 and LY100 structural steel members are chosen for beams, columns and BRBs respectively. The material model of steel is defined as “steel02” in OpenSees and the hysteresis constitutive model of steel is shown in Fig. 2. The parameters of the hysteresis constitutive model of steel are listed in Table 2.

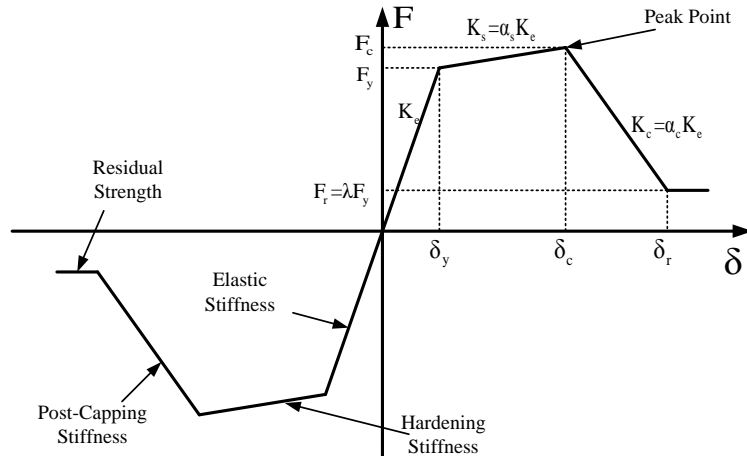


Figure 2 The hysteretic constitutive model of steel: backbone curve

Table 2 Parameters of the hysteresis constitutive model of steel

Steel	Elastic stiffness $K_e$ (MPa)	Yielding strength $F_y$ (MPa)	$\alpha_s$	Strain hardening stiffness $K_s$ (MPa)	Maximum strength $F_c$ (MPa)	Ductility ratio $\delta_c / \delta_y$	$\alpha_c$	Degenerated stiffness $K_c$ (MPa)	$\lambda$	Residual strength $F_r$ (MPa)
A36	200,000	248	0.03	6000	389	20	0.03	-6000	0.2	50
A588	200,000	345	0.03	6000	469	13	0.03	-6000	0.2	69
LYP100	200,000	122	0.06	12000	737	85	0.01	-2000	0.4	49

The results from Ref. [18] are used to calibrate the FE model in this study. The comparison of the main results from Ref. [18] and the FE model developed by OpenSees is listed in Table 3. It can be seen that a good agreement is achieved which proves the validity of the FE model.

Table 3 Comparison of structural responses

Amplitude ratios of peak values of El Centro earthquake ground motion	0.5		1.0		1.5	
	Ref. [13]	OpenSees	Ref. [13]	OpenSees	Ref. [13]	OpenSees
Maximum displacement / m	0.200	0.169	0.385	0.276	0.488	0.336
Maximum story drift angle / %	0.857	0.730	1.509	1.150	2.131	1.730

Maximum story speed / m/s	0.835	0.805	1.381	1.309	1.469	1.461
Maximum story acceleration / m/s <sup>2</sup>	3.288	3.235	5.415	6.302	6.146	8.867
Maximum base shear / MN	11.581	9.590	17.337	15.369	19.400	17.137

### 2.3 Analysis methods

To investigate the collapse resisting capacity, incremental dynamic analysis (IDA) is conducted. The 5% damped spectral acceleration  $S_a(T_1, 5\%)$  at the fundamental period  $T_1$  is used for the original spectral acceleration, which is amplified gradually in IDA method.

During the analysis, if the drift of a column exceeds 10%, it will be judged as failure and would be removed in Opensees model [19]. The removal criterion of BRBs is based on steel material property of LYP100 [20]. In that case, when the axial displacement of BRB is larger than 24 times of the yield displacement, the corresponding BRB component would be removed. It should be mentioned that low-cycle fatigue criterion is not used in this study which is because that the failure of BRB under large deformation in collapse analysis differs from the fatigue failure of BRB under earthquake. The failure of BRB under large deformation is more likely caused by the fracture of the core unit in BRB.

## 3. COLLAPSE RESISTANCE AND FRAGILITY ANALYSIS UNDER SEISMIC LOAD

### 3.1 Collapse resistance analysis under seismic load using random IDA

#### 3.1.1 No component-removal analysis using random IDA

Three models, namely steel frame (SF), BRB frame1 (BRBF1) and BRB frame2 (BRBF2), are analyzed using random IDA method with the seismic input of 20 selected ground motion records listed in Table 4. Based on the research of Ref. [21], earthquake magnitude, epicentral distance and PGA are considered when selecting the ground motions.

Table 4 Details of earthquake ground motions

Serial numbers of ground motions	Earthquake events	Seismic stations	Direction
GM-1	Duzce, Turkey 1999-11-12	Bolu	000
GM-2	Cape Mendocino 1992-4-25 18:06	89324 Rio Dell Overpass-FF	360
GM-3	Northridge 1994-1-17 12:31	90013 Beverly Hills-14145 Mulhol	009
GM-4	Chi-Chi, Taiwan 1999-9-20	CHY101	W
GM-5	Northridge 1994-1-17 12:31	90054 LA-Centinela Station	245
GM-6	Loma Prieta 1989-10-18 0:05	1601 Palo Alto-SLAC Lab	360
GM-7	Loma Prieta 1989-10-18 0:05	1002APEEL 2 Redwood C	133

GM-8	Imperial Valley 1979-10-15 23:16	6610 Vitoria	345
GM-9	Northridge 1994-1-17 12:31	14368 Downey Co Maint Bldg	090
GM-10	Chi-Chi, Taiwan 1999-9-20	CHY015	E
GM-11	Morgan Hill 1984-4-24 21:15	47380 Gilroy Array #2	090
GM-12	Morgan Hill 1984-4-24 21:15	47381 Gilroy Array #3	000
GM-13	Livermore 1980-1-24 19:00	57187 San Ramon Eastman Kodak	180
GM-14	Point Mugu 1973-2-21 14:45	272 Port hueneme	180
GM-15	Whittier Narrows 1987-10-1 14:42	90081 Carson-Water St	180
GM-16	Coalinga 1983-5-2 23:42	36226 Parkfield Cholame 8W	270
GM-17	Whittier Narrows 1987-10-1 14:42	14395 LB-Harbor Admin FF	090
GM-18	N. Plam Springs 1986-7-8 9:20	5067 Indio	225
GM-19	Whittier Narrows 1987-10-1 14:42	90038 Torrance-W 226th St	180
GM-20	Livermore 1980-1-24 19:00	57063 Tracy Sewage Treatm plant	093

The IDA analysis results in Fig. 3 show that the median collapse capacity of SF is 1.37g and logarithmic standard deviation of SF is 0.50g. The median collapse capacity of BRBF1 and BRBF2 are 8.94g and 7.97g, respectively, and logarithmic standard deviation of BRBF1 and BRBF2 are 0.38g and 0.32g, respectively. Due to the contribution of BRB components, the horizontal collapse resisting capacity of the structure is improved, and the earthquake energy is dissipated significantly. The median collapse capacity of BRBF2 is 11.4% larger than that of BRBF1, which indicates that the horizontal collapse resisting capacity of BRBF2 is greater than that of BRBF1. The reason for enhanced collapse resisting capacity is that the cross BRBs are arranged in BRBF2 so the axial forces of BRBs could be transferred continuously. Meanwhile, no imbalanced shear force is to be resisted in the beams and columns.

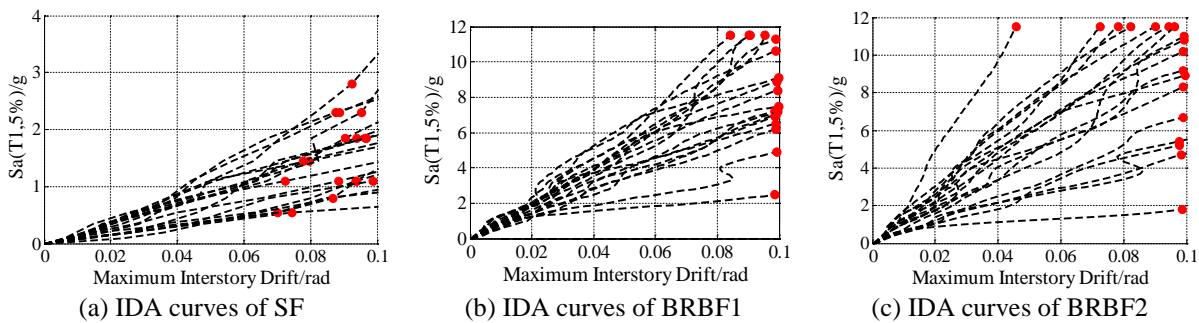


Figure 3 IDA curves and collapse points based on No component-removal random IDA

### 3.1.2 Component-removal analysis using random IDA

Since no component-removal analysis would not reflect the dynamic effect caused by suddenly removal of critical components, component-removal analysis is executed in this section. The bottom columns and BRBs in axis A, axis B and axis C are removed from three models, one component at each time.

The IDA curve results in Fig. 4 show that median collapse capacity of BF is 1.30g and logarithmic standard deviation of BF is 0.58g. Meanwhile the median collapse capacity of BRBF1 and BRBF2 are 6.34g and 7.67g, respectively, and logarithmic standard deviation of BRBF1 and

BRBF2 are 0.39g and 0.36g. Compared with IDA results of BF and BRBF1, median collapse capacity of BRBF1 is 3.88 times of that of BF, and the median collapse capacity of BRBF2 is 4.9 times larger than that of BF. It can be observed that with the contribution of the BRBs, horizontal collapse resistance of the structure was significantly improved and the variation of the resistance is decreased.

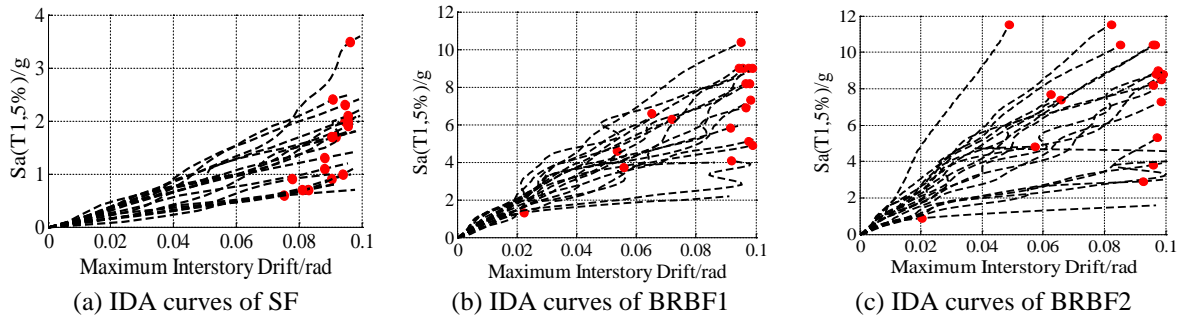


Figure 4 IDA curves and the points of collapse based on component-removal random IDA

### 3.2 Failure modes of structural systems

Based on incremental dynamic analysis (IDA) method, the plastic hinges development and the failure modes of steel frame, asymmetric BRB steel frame and symmetric BRB steel frame would be analyzed using non-removal analysis.

#### 3.2.1 Steel frame (SF)

There are three main failure modes of steel frame (SF) observed, which are roof-failure mode, 2nd floor failure mode and 3rd floor failure mode, as shown in Fig. 5. The occurrence ratio of three failure modes is 60.4%, 14.3% and 19.7%, respectively. Roof-failure mode, which is the dominant modes, featured with plastic hinges formed in the beams on 8th and 9th floors and columns on 8th floor. The plastic hinge on 8th floor columns results in the collapse of 8th or 9th floor. The 2nd floor failure mode is the failure of the columns on 2nd floors which results in the collapse of superstructure. The 3rd floor failure mode is similar with the failure mode of 2nd floor.

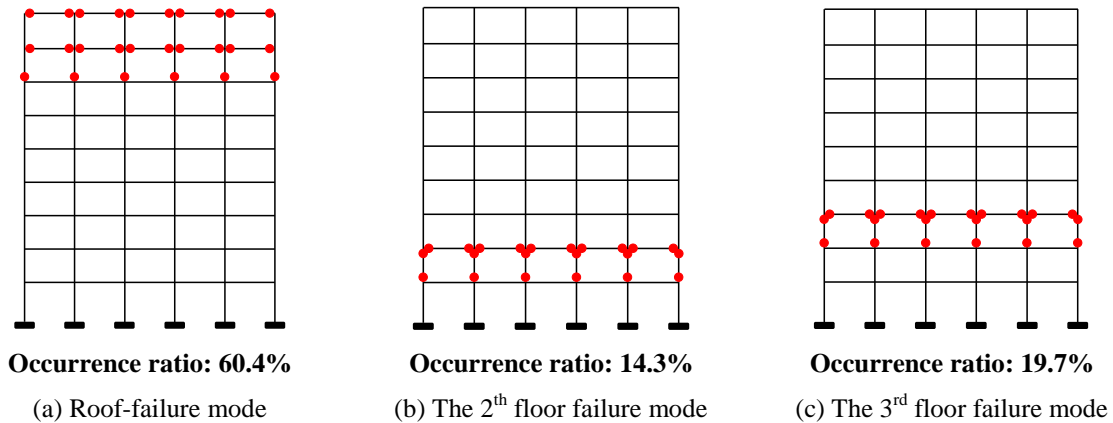


Figure 5 Three main failure modes of SF

3.2.2 Asymmetric BRB steel frame (BRBF1)

There are four failure modes in BRBF1 with asymmetrical arrangement of BRBs, which are whole-BRBs-failure mode, roof-BRBs-failure mode, mid-floors-BRBs-failure mode and BRBs-columns-failure mode. As shown in Fig. 6, the occurrence ratios of four modes are 60.5%, 11.4%, 23.7% and 2.6%, respectively. The first mode is whole-BRBs-failure mode that all BRB components fail. In that case, no energy dissipation components left and building failed due to strong earthquakes. The whole-BRBs-failure mode is the dominant failure mechanics of the structure, in which the structure has the largest energy consumption. The second failure mode is the failure of the BRBs on roof stories. In this case, the main structure loses the protection from the BRBs in roof stories under earthquake. The third failure mode is similar to the second failure mode but the BRBs fail at 3<sup>rd</sup> and 4<sup>th</sup> floor. The last failure mode is that the drift of column B in 3<sup>rd</sup> floor exceeds 10% after all BRBs fail, so that the main structure collapses after the column B fails. The last failure mode is very rare as it requires significant large energy dissipation capacities of structural components.

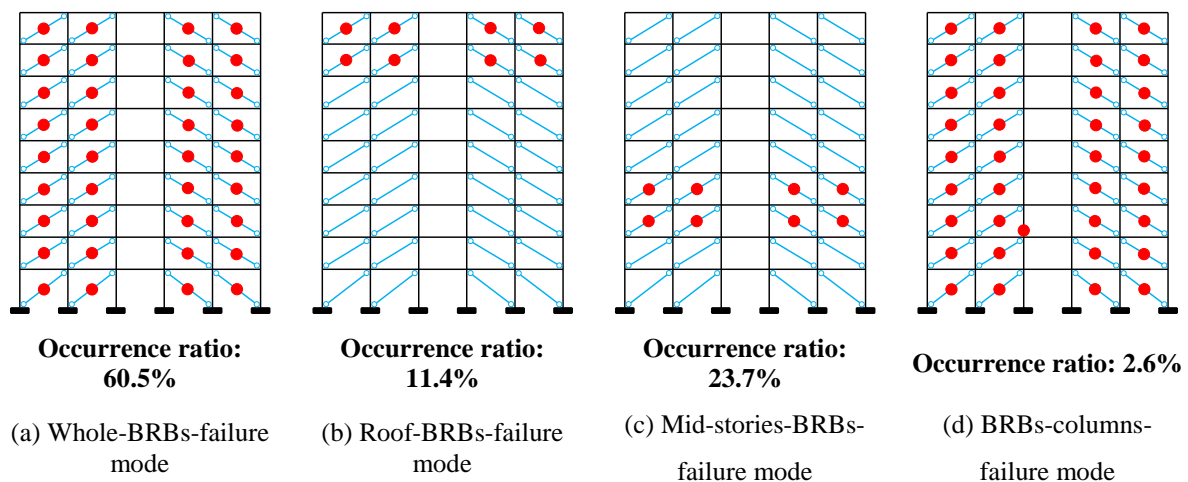


Figure 6 Four failure modes of BRBF1

3.2.3 Symmetric BRB steel frame (BRBF2)

Three failure modes in BRBF2 with symmetrical arrangement of BRBs are shown in Fig. 7. The failure modes are whole-BRBs-fail mode, roof-BRBs-fail mode and mid-floors-BRBs-fail mode. The occurrence ratios of three modes are 62.2%, 11.7% and 24.3%, respectively. Failure mechanism of the three modes is similar with the former three failure modes of BRBF1.

In fact, the failure mode of the steel frame structure with BRBs is expected to be the mode of whole BRBs failure, and the analysis results prove the expectations. Most of BRB components absorb the earthquake energy and fail preceding the beams and columns, so that the main structure can be

protected from the strong earthquake ground motions effect and suffer less seismic damage. It could be seen that two kinds of BRB steel frame structures designed in this paper exhibit good anti-collapse capacity and energy consumption capacity.

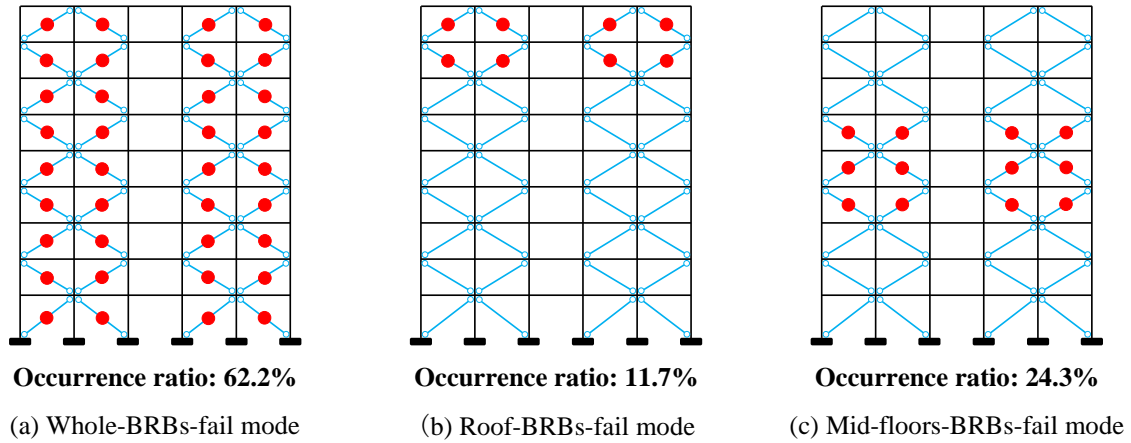
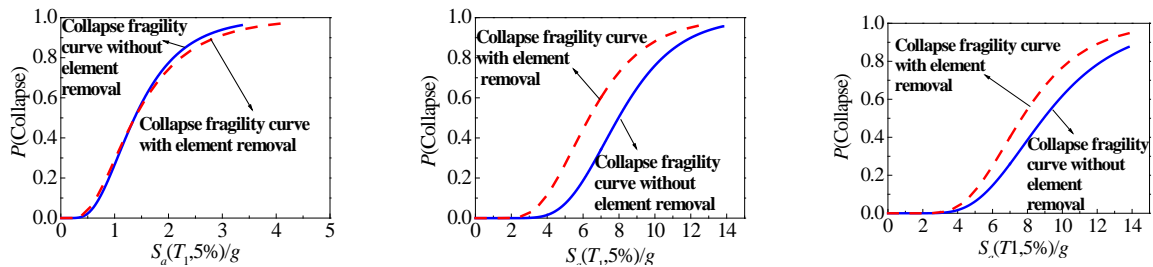


Figure 7 Three main failure modes of BRBF2

### 3.3 Fragility analysis of collapse resistance under seismic load

In fragility analysis, SF, BRBF1 and BRBF2 are analyzed in two cases: no component removal and critical component removal. Based on two types of random IDA methods, the median and logarithmic standard deviation of horizontal collapse resisting capacity are assessed, and then the structural collapse fragility is obtained. The fragility results of the three structures are shown in Table 5 and Fig. 8.



(a) Fragility curves comparison of BF (b) Fragility curves comparison of BRBF1 (c) Fragility curves comparison of BRBF2

Figure 8 Comparison of fragility curves between no components removal and critical components removal schemes

Table 5 Median and logarithmic standard deviation of horizontal collapse fragility function

Structures	No removal		Critical components removal		Difference/%	
	Median	Logarithmic standard deviation	Median	logarithmic standard deviation	Median	logarithmic standard deviation
SF	1.37 g	0.5 g	1.30 g	0.58 g	5.1 g	16 g
BRBF1	7.97 g	0.32 g	6.34 g	0.39 g	20.5 g	21.9 g

BRBF2    8.93 g            0.38 g            7.67 g            0.36 g            14.1 g            5.3 g

As shown in Fig. 9, the horizontal collapse conditional failure probability of SF is larger than BRBFs. The load transferring paths of BRBs in BRBF2 is more efficient, so the fragility curves of BRBF2 are below of those of BRBF1, which indicates that the collapse resisting capacity of BRBF2 is better than that of BRBF1.

From the comparison of fragility results, it can be seen that the structural fragility of SF is similar based on two IDA methods. However the existence of BRBs leads to a great increase in the collapse resistance of structures. It is shown that the importance of BRBs for improving the collapse resistance of structures.

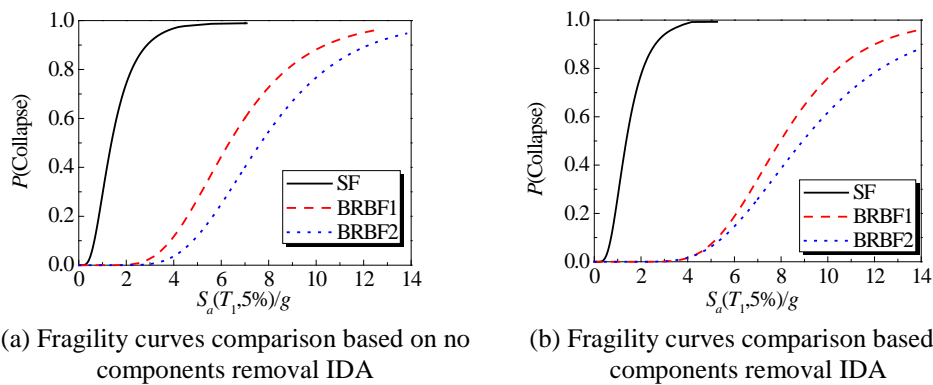
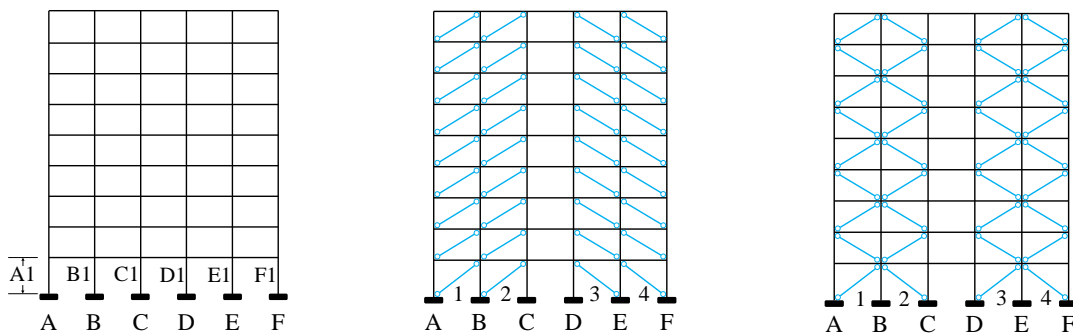


Figure 9 Comparison of fragility curves between three structural systems

#### 4. COLLAPSE RESISTANCE AND FRAGILITY ANALYSIS UNDER DYNAMIC COMPONENT-REMOVAL

##### 4.1 Collapse analysis under dynamic component-removal using APM

Based on alternative path method (APM), collapse analysis is conducted considering the scenario of critical component removal. APM is an event-independent analysis method which does not consider the reason of critical structural component failure. This method focuses on the response of the remaining structure. The serial numbers of the removal components are shown in Fig. 10.



(a) Steel frame                      (b) Asymmetric BRB steel frame                      (c) Symmetric BRB steel frame

Figure 10 Elevation view of three structures

The schemes of APM for three models are shown in Table 6. Considering the symmetry of the structure, three kinds of component removal schemes are considered in dynamic analysis.

Table 6 Schemes of APM

APM	Removal schemes of steel frame	Removal schemes of BRB steel frame
I	Column A1	Column A1, BRB1
II	Column B1	Column B1, BRB1, BRB2
III	Column C1	Column C1, BRB2

APM I: Column A1 is removed from bare steel frame while column A1 and BRB1 are removed from buckling-restrained braced steel frame;

APM II: Column B1 is removed from bare steel frame while column B1, BRB1 and BRB2 are removed from buckling-restrained braced steel frame;

APM III: Column C1 is removed from bare steel frame while column C1 and BRB2 are removed from buckling-restrained braced steel frame.

There are three steps of nonlinear dynamic column-removal analysis: 1) Apply gravity loads on all structural components; 2) Remove the critical components; 3) Apply unbalanced loads on the structure in the reverse direction and conduct a dynamic analysis. Because the critical components are abruptly removed, the unbalanced load is an instantaneous increase of rectangular-shaped load. The loading diagrams are shown in Fig. 11.

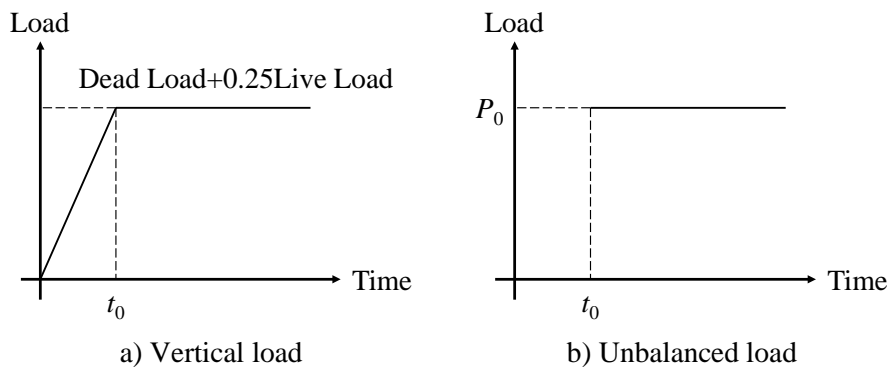


Figure 11 Two kinds of loads

Based on ASCE 7-10 (2010), the minimum live load on various buildings is 2.5 kN/m<sup>2</sup>. Hence, the load combination of the first story is 54.71 kN/m, from the second story to the eighth story whose load combination is 53.81 kN/m and the load combination of the ninth story is 57.28 kN/m.

#### 4.1.1 APM I

As shown in Fig. 12, the maximum vertical displacement of steel frame is 9.24 cm in the nonlinear dynamic analysis of APM I. After installing BRBs, the maximum vertical displacements of BRBF1 and BRBF2 are 3.67 cm and 3.08 cm, which are reduced by 60.3% and 66.7% respectively. It seems reasonable that the progressive collapse capacity and the stiffness of the structures are improved due to the contribution of the BRBs.

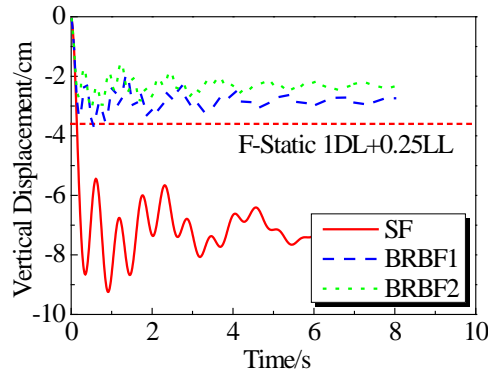
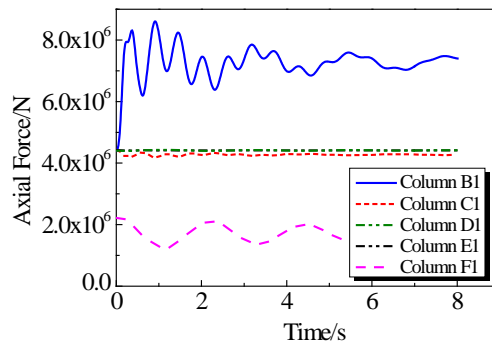
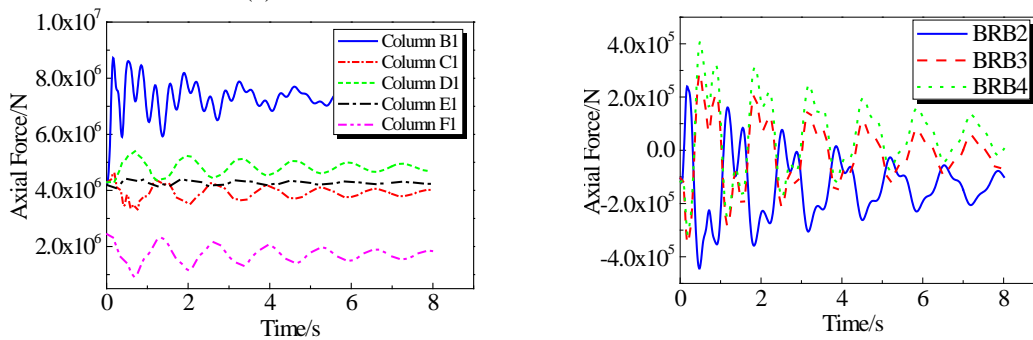


Figure 12 Structural responses in APM I

As shown in Fig.13, after the bottom column A1 is removed, and the internal forces of remaining components are redistributed. In steel frame, internal force of column B1 is increased from 4405 kN to 8603 kN. The axial forces of column C1, D1, E1 and F1 remain unchanged in the whole process. For the BRB steel frames, internal force variation tendency of the remaining columns is similar with that of the steel frame. The axial force variation of BRB2 component is large, and the internal forces of the BRB3 and BRB4 are altered from compression to tension.



(a) Axial force redistribution of bottom column in SF



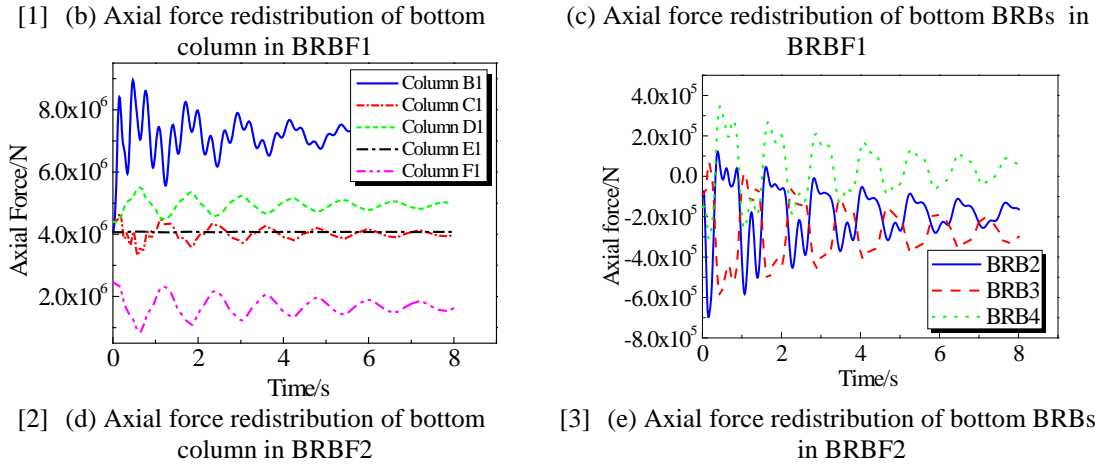


Figure 13 Load redistribution of bottom components of different structures in APM I

Table 7 shows the maximum axial force variation of remaining bottom components of three models. The axial forces of the remaining components did not exceed the ultimate strength during the whole analysis. The variation ratios of the BRBs are between 319% and 752%, which indicates that BRBs greatly enhance the redistribution capacity of internal force in the models.

Table 7 Maximum axial forces variation of residual bottom components of three structures in APM I

Structures	Col B1	Col C1	Col D1	Col E1	Col F1	BRB2	BRB3	BRB4	
SF	Before removal / kN	4405	4408	4400	4423	2208	-	-	-
	After removal / kN	8603	4423	4424	4431	2217	-	-	-
	Variation Ratios / %	95.3%	0.34%	0.54%	0.18%	0.41%	-	-	-
BRBF1	Before removal / kN	4213	4292	4260	4191	2429	106	105	118
	After removal / kN	8721	4643	5399	4438	2441	444	-348	-407
	Variation Ratios / %	107%	8.2%	26.7%	5.9%	0.5%	319%	431%	445%
BRBF2	Before removal / kN	4095	4399	4401	4066	2429	87.5	90.6	152
	After removal / kN	8950	4674	5505	4095	2451	697	-591	-347
	Variation Ratios / %	119%	6.3%	25.1%	0.71%	0.91%	697%	752%	328%

4.1.2 APM II

In the nonlinear dynamic analysis of APM II, column B1 in steel frame model is removed and column B1, BRBF1 and BRBF2 in two BRBF models are removed. As shown in Fig. 14, the maximum vertical displacement of the steel frame is 7.21 cm. The maximum vertical displacement of BRBF1 and BRBF2 are 2.73 cm and 2.20 cm, which are decreased by 62.1% and 69.5%, respectively.

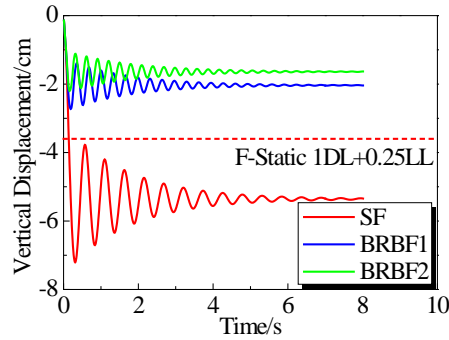
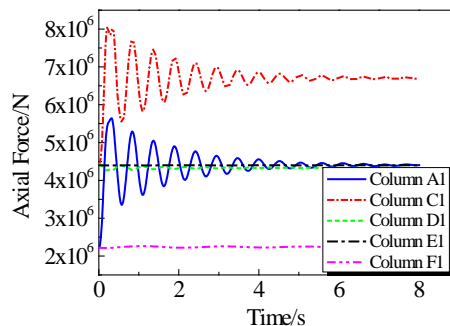


Figure 14 Structural responses in APM II

Compared with the APM I, it can be noticed that vertical displacement time history curves of the models in APM II are more stable. The reason is that the bottom story horizontal vibration of the structure is very small after the removal of the left center column. On the contrary, the structure becomes asymmetric after the removal of left side column in APM I and the structural asymmetry would cause significant horizontal vibration in the models.

Fig. 15 shows the redistribution of internal forces in bottom remaining components after the removal of critical components. The maximum axial force variations of the remaining components are calculated in Table 8. In steel frame, the axial force of column A1 which is the nearest component to column B1 increases from 2222 kN to 5639 kN while the axial force of column C1 increases from 4427 kN to 8046 kN. It is concluded that after the removal of column B1, the internal forces of column B1 are transferred to other adjacent components. The axial forces of columns D1, E1 and F1 which are far away from the column B1 remain unchanged in the analysis process.



(a) Axial force redistribution of bottom column in SF

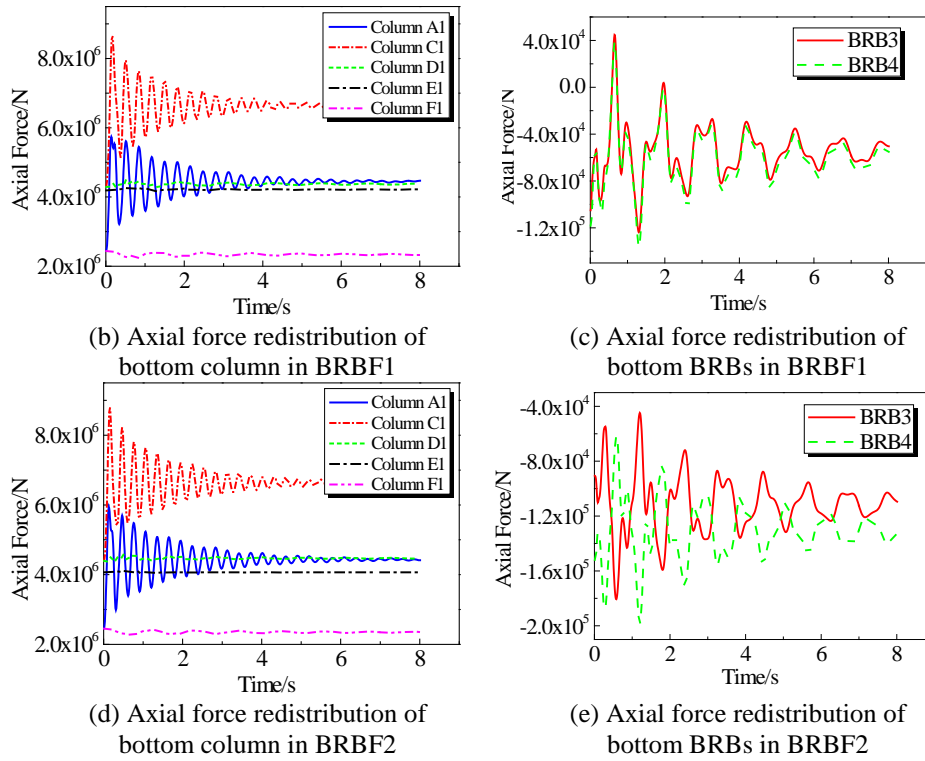


Figure 15 Load redistribution of bottom components of different structures in APM II

Table 8 Maximum axial forces variation of residual bottom components of three structures in APM II

Structures	Col A1	Col C1	Col D1	Col E1	Col F1	BRB3	BRB4	
SF	Before removal / kN	2222	4427	4293	4423	2217	-	-
	After removal / kN	5639	8046	4422	4403	2263	-	-
	Variation Ratios / %	154%	81.7%	3%	0.45%	2.1%	-	-
BRBF1	Before removal / kN	2441	4313	4293	4192	2441	105	118
	After removal / kN	5739	8665	4499	4275	2443	124	136
	Variation Ratios / %	135%	101%	4.8%	2%	0.1%	18.1%	15.3%
BRBF2	Before removal / kN	2461	4406	4398	4066	2450	92	152
	After removal / kN	5940	8784	4572	4104	2453	181	198
	Variation Ratios / %	141%	99.4%	4%	0.9%	0.1%	96.7%	30.3%

In BRB steel frames, the internal force variation tendency of bottom remaining columns is similar with that of the steel frame after the sudden removal of bottom column B1, BRB1 and left

BRB2. The axial forces of remaining components do not exceed their ultimate strength in dynamic response process in APM II.

4.1.3 APM III

In APM III, column C1 in steel frame model is removed while column C1 and BRB2 in two BRBF models are removed, Fig. 16 shows that the maximum vertical displacement of the SF is 7.18 cm. The maximum vertical displacements of BRBF1 and BRBF2 are 4.36 cm and 4 cm respectively, which are 39.3% and 44.3% lower than that of the SF. The decrease of the vertical displacement of BRBFs in APM III is relatively smaller than that of APM II.

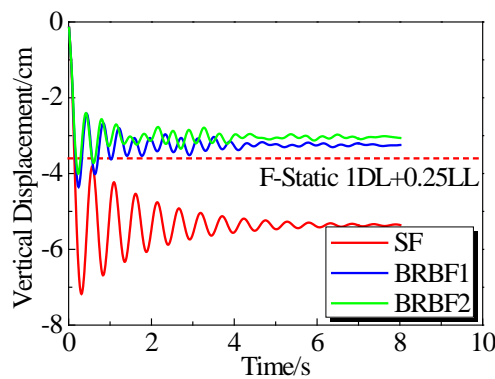
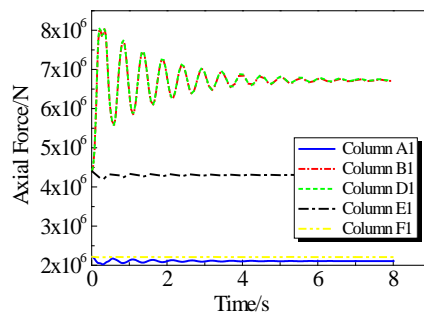
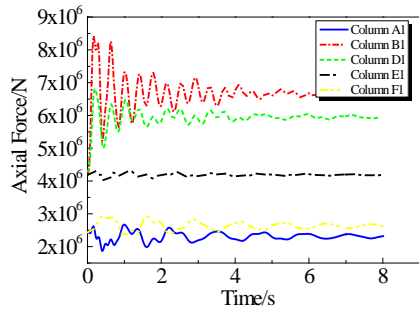


Figure 16 Structural responses in APM III

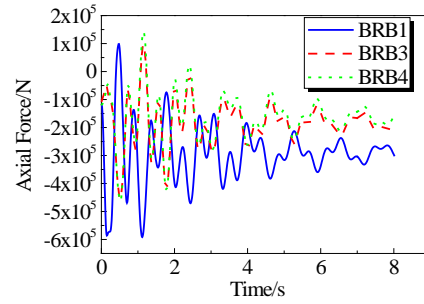
Similarly, the internal forces redistribution curves of bottom remaining components are shown in Fig. 17 and Table 9. In steel frame, the axial force of column B1 which is the nearest component to column C1 is increased from 4404 kN to 8034 kN, and the axial force of column D1 is increased from 4427 kN to 8046 kN. The increment of axial forces implies that the internal force of column A1 is transferred to the adjacent components after the removal of column A1. The axial forces of column E1 and F1 which are far away from the column D1 remain unchanged in the whole process.



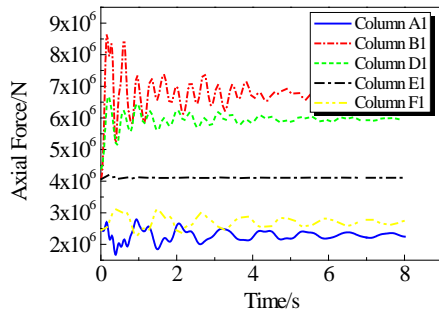
[4] (a) Axial force redistribution of bottom column in SF



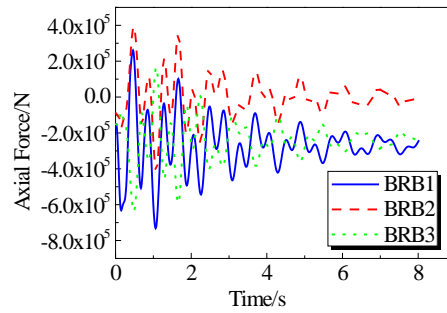
[5] (b) Axial force redistribution of bottom column in BRBF1



[6] (c) Axial force redistribution of bottom BRBs in BRBF1



[7] (d) Axial force redistribution of bottom column in BRBF2



[8] (e) Axial force redistribution of bottom BRBs in BRBF2

Figure 17 Load redistribution of bottom components of different structures in APM III

Table 9 Maximum axial force variation of residual bottom components of three structures in APM III

Structures	Col A1	Col B1	Col D1	Col E1	Col F1	BRB1	BRB3	BRB4
SF	Before removal / kN	2213	4404	4227	4389	2216	-	-
	After removal / kN	2216	8034	8046	4400	2217	-	-
	Variation Ratios / %	0.13%	82.4%	90.3%	0.25%	0.1%	-	-
BRBF1	Before removal / kN	2440	4197	4297	4191	2441	119	105
	After removal / kN	2671	8420	6820	4326	2928	592	453
	Variation Ratios / %	9.5%	101%	58.7%	3.2%	20%	397%	331%
BRBF2	Before removal / kN	2450	4085	4403	4066	2450	151	90.6
	After removal / kN	2790	8644	6676	4189	3120	732	411
	Variation Ratios / %	13.9%	112%	51.6%	3%	27.3%	384%	354%

The internal force variation tendency of bottom remaining columns in BRBFs is similar with that of the SF while the bottom column C1 and BRB2 are removed. The internal forces variations of BRBs

are evident, which indicate that BRBs enhance the redistribution capacity of internal force. The axial forces of remaining components do not exceed the ultimate stress in analysis process in APM III.

4.2 Collapse analysis under dynamic component-removal using IDA method

To investigate the failure modes under the condition of critical components removal, incremental dynamic analysis (IDA) method [22-24] is adopted. The amplification factor  $\alpha$  of the combined load is used to adjust the applied loads, which equal to  $\alpha$  (Dead load + 0.25 Live load).

Firstly, the equivalent load  $\alpha$  (Dead load + 0.25 Live load) is applied to all spans. Secondly, for the spans in which the columns have been removed, the factor  $\alpha$  of the equivalent load is amplified larger than 1. Finally, the load factor  $\alpha$  is increased step by step considering of vertical dynamics effect until the structures collapse.

4.2.1 APM I

Fig. 18 shows the plastic hinges development of SF, BRBF1 and BRBF2 in APM I. With the left side column removal, the plastic hinges occur at the beam end of the steel frame, which are far away from the location of removal column and are further distributed to the upper stories. In BRBF1, failure firstly appears at the BRB components which locate at the left side span of the top story. The failure of the BRBs spreads to the lower stories and beam hinges formed. In BRBF2, the failure tendency of the structure is the same as that of BRBF1, but the beam hinges do not occur at every story, it only appears at the central and bottom stories. The beam hinge amount of the BRBF2 is less than that of SF and BRBF1.

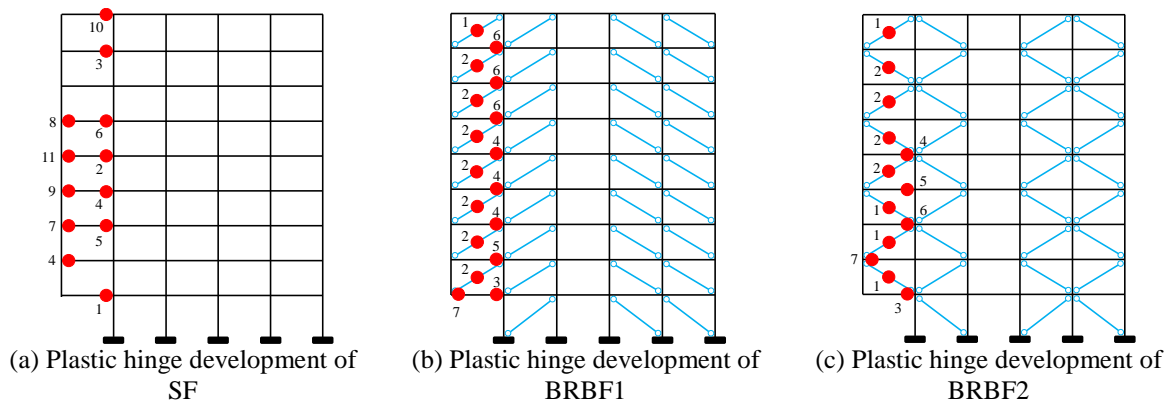


Figure 18 Plastic hinge development of three structures in APM I

The load distribution paths in BRB components are very consistent in two BRB frames. Once the failure of the bottom columns happens, BRB components play the role of enabling alternative load path while the beam and column elements are well protected. The failure of the whole structure would not happen in this scheme.

Fig. 19 shows the vertical IDA curves of different models. The maximum load factors in three structures are 1.78, 2.39 and 2.48, respectively. The maximum vertical displacements of three structures are 48.15 cm, 36.1 cm and 29.5 cm. With the contribution of the BRBs, the loading bearing capacity of the structures is increased while the deformation ability of the structures is decreased.

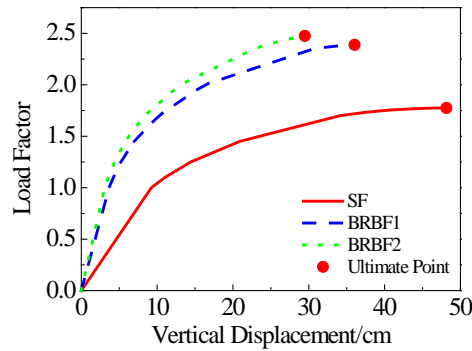


Figure 19 Vertical displacements of three structures in APM I

#### 4. 2.2 APM II

Fig. 20 shows the plastic hinge development of SF, BRBF1 and BRBF2 in APM II. When the left central column is removed, the plastic hinges in SF appears at the beam ends in the top story, and the plastic hinges spread to the adjacent beam ends where is far away from the joint of the removed column. In BRBF1, the failure starts at the BRB components which locate in the span of the removed column, and spreads to the adjacent beam ends. In BRBF2, the failure starts at the BRB components which locate in the central stories and spread to upper stories.

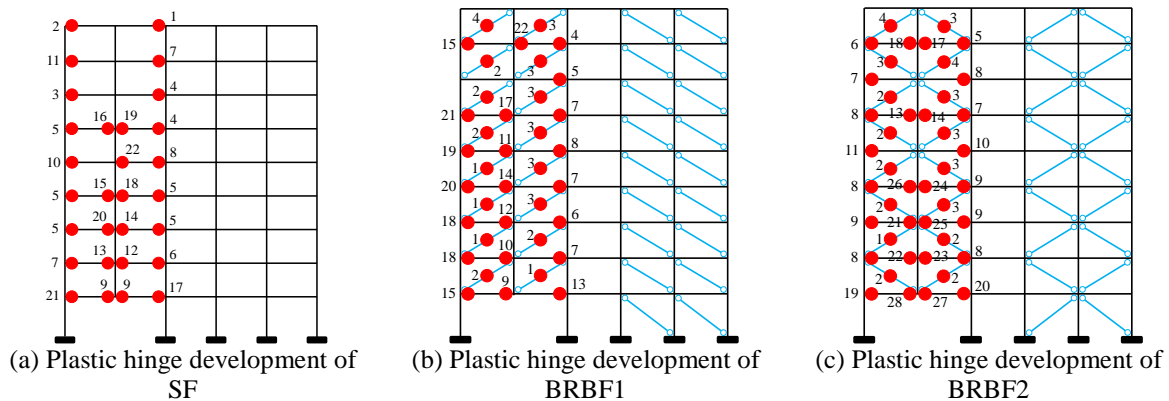


Figure 20 Plastic hinge development of three structures in APM II

Fig. 21 shows the different vertical IDA curves of three structures. The maximum load factors of three structures are 1.81, 2.41 and 2.58, respectively. The maximum vertical displacements of three structures are 46.6 cm, 35.9 cm and 36.2 cm. The trend of the vertical displacements of three structures in APM II is similar with that in the APM I. The maximum vertical displacement of BRBF2

is larger than that of BRBF1, which indicates that BRBF2 has larger collapse resisting capacity than BRBF1 under the condition of APM II. Since BRBF2 has a more coherent load transmission path for structural components than SF and BRBF1, the load of the structure can be efficiently transferred to more remaining structural components.

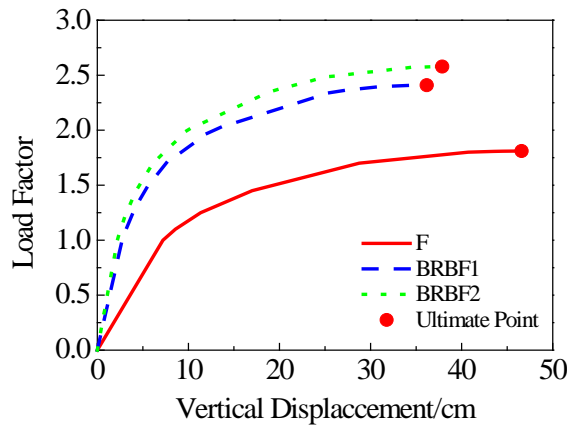


Figure 21 Vertical displacements of three structures in APM II

4. 2.3 APM III

Fig. 22 shows the plastic hinge development of steel frame, BRBF1 and BRBF2 in APM III. For steel frame, plastic hinges starts to form at the far ends of beam where is far away from the removed column element. When the plastic hinge occurs on the far end of beam in the fourth floor, the structure collapses.

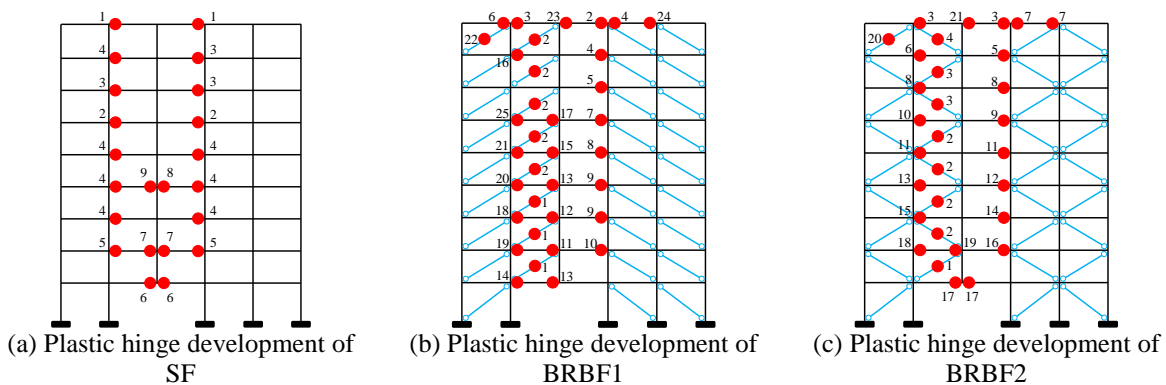


Figure 22 Plastic hinge development of three structures in APM III

The BRB components are not installed at the middle span. Therefore plastic hinges first appear at the beams in inner spans. In APM III, the amount of hinges is significantly less than that in APM II. Under the condition of the bottom central column being removed, the plastic hinge distributions and collapse resisting capacity of the two structures are similar.

Fig. 23 shows the vertical IDA curves of structures. The maximum load factors of three structures are 1.81, 2.10 and 2.16, respectively. The maximum vertical displacements of three structures are 46.2 cm, 37.6 cm and 38.1 cm, respectively. The maximum vertical displacements and load factors of BRBF2 are similar with those of BRBF1, which indicates that two BRBF models have the similar collapse resisting capacity under the condition of APM III.

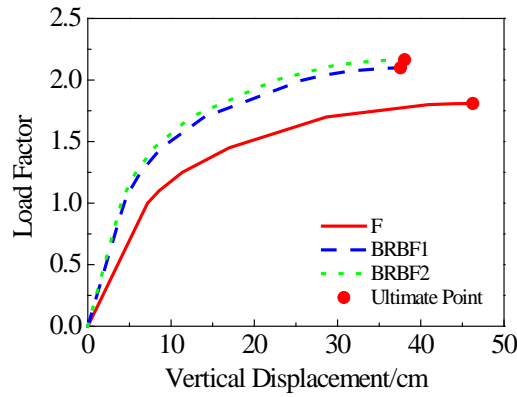


Figure 23 Vertical displacements of three structures in APM III

#### 4.3 Fragility analysis of collapse resistance under dynamic component removal

In this section, the structural performance is analyzed by considering of the uncertainty of steel strength of column  $f_{y,b}$ , steel strength of beam  $f_{y,c}$ , steel inner core strength of BRB elements  $f_{y,br}$ , elastic modulus of steel  $E$  and dead load coefficient. The statistical parameters are listed in Table 10.

Table 10 Statistical parameters of structural uncertainty

Random variable	Mean	Coefficient of variation	Distribution type
$f_{y,c}$	345MPa	0.07	Lognormal
$f_{y,b}$	248MPa	0.07	Lognormal
$f_{y,br}$	100MPa	0.07	Lognormal
$E$	200000MPa	0.02	Lognormal
DL factor	1	0.07	Normal

From the engineering experience, the load uncertainty parameters should be independent from the structural material parameters, while the parameters of steel materials should be dependent of each other. The existing data is not sufficient to obtain a correlation matrix of precise correlation random parameters, whereas the correlation of random variables has a significant impact on the outcome of the uncertainty analysis. In this paper, based on the results of Ref. [25-26], only the correlations among steel material parameters are considered, and other parameter, such as Dead Load (DL) factor is assumed to be independent of each other. The correlation coefficient matrix of uncertain structure parameters is listed in Table 11.

Table 11 Correlation coefficient matrix of structural uncertainty parameters

	$f_{y,c}$	$f_{y,b}$	$f_{y,br}$	$E$	DL factor
$f_{y,c}$	1	0	0	0.3	0
$f_{y,b}$	0	1	0	0.3	0
$f_{y,br}$	0	0	1	0.3	0
$E$	0.3	0.3	0.3	1	0
DL factor	0	0	0	0	1

Based on Latin hypercube sampling, 100 random structural samples are chosen for each structure considering of three APM schemes. The collapse resistance of steel frame and buckling-restrained braced steel frame under component removal are analyzed with the vertical incremental dynamics analysis (IDA) approach. The IDA curves are shown in Fig. 24~26, which are for APM I, APM II and APM III, respectively. Each curve represents the relationship between the vertical displacement and the load coefficient under the random samples of each structure. Taking the collapse fragility as evaluation indices, the probabilistic collapse capacity of steel frame and buckling-restrained braced steel frame is analyzed.

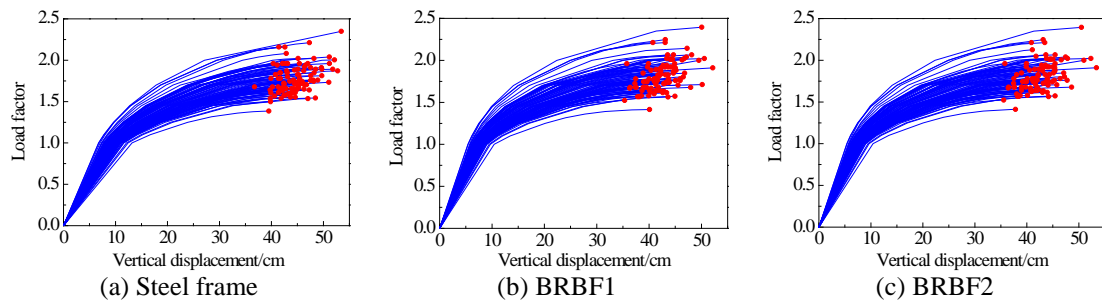


Figure 24 Vertical IDA curves of three structures (APM I)

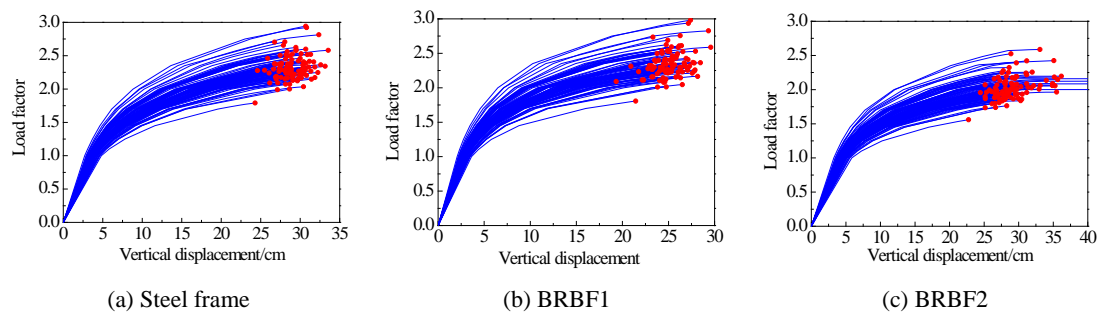


Figure 25 Vertical IDA curves of three structures (APM II)

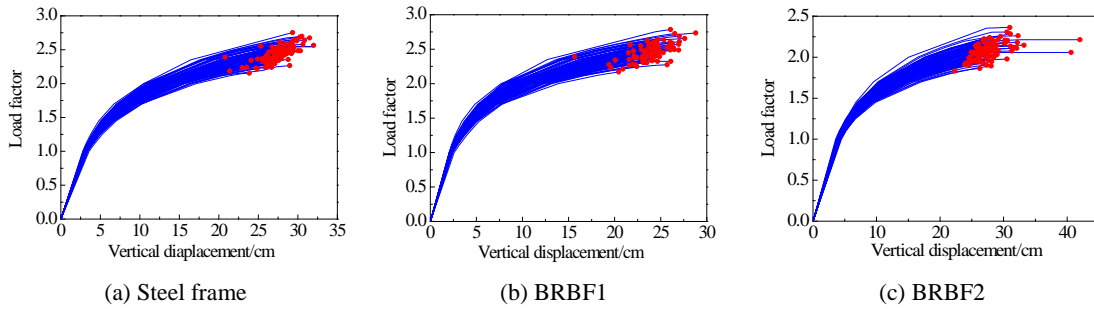


Figure 26 Vertical IDA curves of three structures (APM III)

According to the recommended guideline of GSA 2003, the limit state of structural collapse is determined as section rotation angle of beam element which is 0.21 rad. Based on random IDA analysis, the median  $m_c$  and logarithmic standard deviation  $\beta_c$  of vertical collapse fragility of steel frame and BRBF are identified as shown in Table 12. The lognormal fit fragility curves of steel frame and BRBF can be derived as shown in Fig. 27. The medians of vertical collapse fragility function of BRBFs are larger than those of steel frame, and the logarithmic standard deviations of vertical collapse fragility function of BRBF are less than those of steel frame, which indicates the collapse resistance of BRBF is larger than that of steel frame.

Table 12 Median and logarithmic standard deviation of vertical collapse fragility function

	APM I			APM II			APM III		
	SF	BRBF1	BRBF2	SF	BRBF1	BRBF2	SF	BRBF1	BRBF2
$m_c$	1.76	2.31	2.43	1.79	2.32	2.45	1.79	2.02	2.07
$\beta_c$	0.096	0.070	0.050	0.097	0.073	0.051	0.097	0.077	0.051

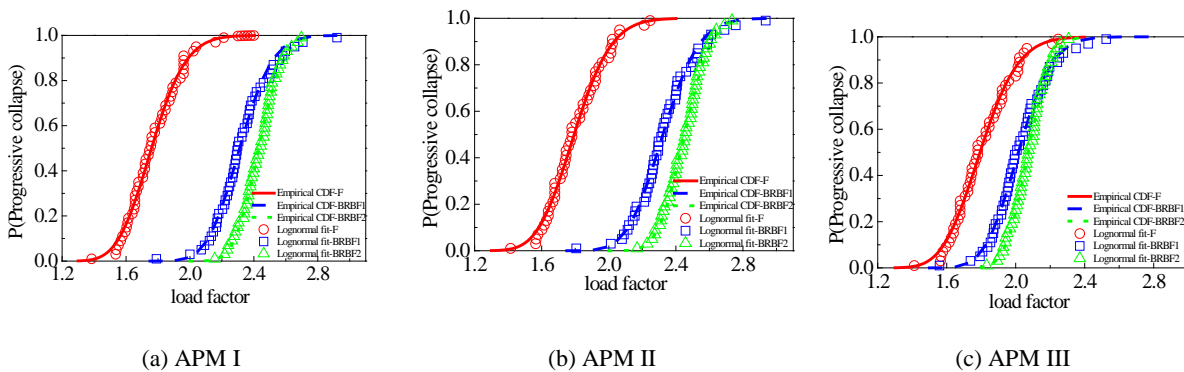


Figure 27 Fragility curves of three schemes for three structures

From the fragility curves derived in section 3.3 and this section, it can be seen that, when BRBs are installed, the failure probability of the structure decreases and the seismic resistance reliability of the structure increases evidently. Buckling-restrained braces provide alternative load paths for structures; hence the structural redundancy is improved. The load transferring paths of BRBs in

BRBF2 are more efficient, therefore the fragility curves of BRBF2 are below those of BRBF1 which indicates that the collapse resistance of BRBF2 is better than BRBF1.

Three schemes of removing components are adopted for collapse analysis. As shown in Fig. 28(a), columns in different positions are removed, which have little effect on the collapse fragility of steel frame. The fragility comparisons of BRBFs are shown in Fig. 28(b)-(c), the fragility curves for APM III are above the other curves, which indicates the scheme of removing column C1 and BRB2 is more critical for BRBF. The collapse resisting capacity is influenced significantly by the column and BRB in the middle spans.

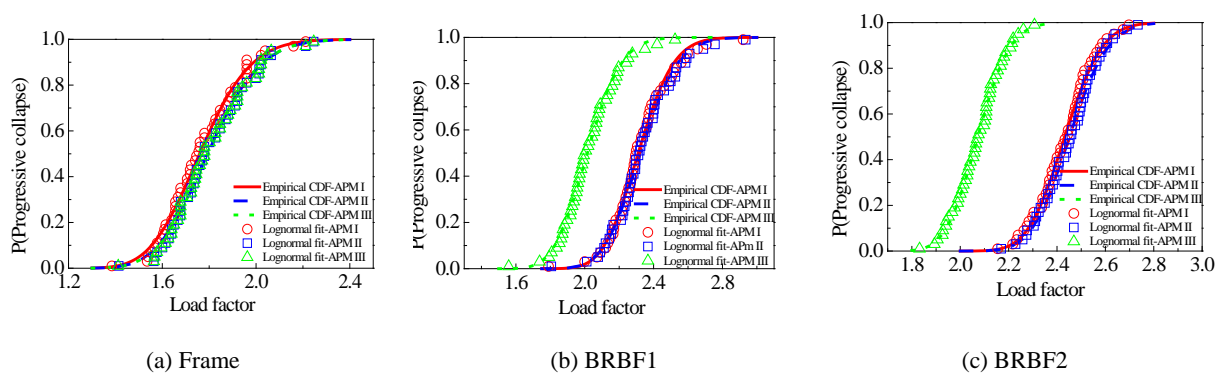


Figure 28 Fragility curves of three structures under three schemes

## 5. CONCLUSIONS

To analyze and compare the collapse resistance of steel frame and buckling-restrained braced frames, the random horizontal and vertical IDA and alternative path method are adopted to study the collapse resisting capacity and collapse fragility of structures. The findings of this study are summarized as follows:

1) Under seismic load, the main collapse mode of SF is roof-failure mode, and the main horizontal collapse failure mode of BRBF is whole BRBs failure mode.

2) Under seismic load, the median collapse capacity of BRBF is about 6 times of that of SF which indicates that the collapse fragility of SF is larger than BRBFs. The collapse fragility of BRBFs considering of component-removal is larger than that of non-component-removal;

3) After installing BRBs, the maximum vertical displacements of SF can be reduced 40%~70%, and the maximum load factors of SF are increased 16%~43% under three APMs. With the alternative load path function of BRBs, the internal force variation of bottom remaining columns of BRBFs is smaller than that of SF, which indicates that BRBs can enhance the internal force redistribution capacity;

4) When the bottom columns are removed, the plastic hinges occur at the beam ends of the steel frame, while the plastic hinges appear at first in the BRBs of BRBFs which provide protection to the main structure.

5) With the contribution of BRBs, the collapse resistance of the structures can be increased and the fragility of the structures can be decreased. The collapse resistance of BRBF2 is better than that of BRBF1 due to the more load transferring paths of BRBs in BRBF2.

## ACKNOWLEDGMENTS

The project is supported by National Natural Science Foundation of China (No. 51008090, No. 51908085) and Xijing University Special Foundation (XJ17T07) which are gratefully acknowledged.

## REFERENCES

- [1] GSA. (2003), "Progressive collapse analysis and design guidelines for new federal office buildings and major modernization projects". The U.S. General Services Administration.
- [2] Unified Facilities Criteria of Department of Defense (UFC-DoD). Design of Buildings to Resist Progressive Collapse, The U.S. Department of Defense, 2005.
- [3] Kim J., Kim T. Assessment of progressive collapse-resisting capacity of steel moment frames. *Journal of Construction Steel Research*, 2009, 65: 169-179.
- [4] Khandelwal K., El-Tawil S. and Sadek F. Progressive collapse analysis of seismically designed steel braced frames. *Journal of Construction Steel Research*, 2009, 65: 699-708.
- [5] Hariri-Ardebili M. A., Sattar S. and Estekanchi H. E. Performance-based seismic assessment of steel frames using endurance time analysis. *Engineering Structures*, 2014, 69: 216-234.
- [6] Kim T., Kim J. and Park J. Investigation of progressive collapse-resisting capability of steel moment frames using push-down analysis. *Journal of Performance of Constructed Facilities*, 2009, 23(5): 327-335.
- [7] Mahdavi-pour M. A. and Deylami A. Probabilistic assessment of strain hardening ratio effect on residual deformation demands of Buckling-Restrained Braced Frame. *Engineering Structures*, 2014, 81: 302-308.
- [8] Eletrabi H. and Marshall J. D. Catenary action in steel framed buildings with buckling restrained braces. *Journal of Constructional Steel Research*, 2015, 113: 221-233.
- [9] Wongpakdee N., Leelataviwat S., Goel S. C., et al. Performance-based design and collapse evaluation of buckling-restrained knee braced truss moment frames. *Engineering Structures*, 2014, 60: 23-31.

- [10] Freddi F., Tubaldi E., Ragni L., et al. Probabilistic performance assessment of low-ductility reinforced concrete frames retrofitted with dissipative braces. *Earthquake Engineering & Structural Dynamics*, 2013, 42: 993-1011.
- [11] Dyanati M., Huang Q. and Roke D. Seismic demand models and performance evaluation of self-centering and conventional concentrically braced frames. *Engineering Structures*, 2015, 84: 368-381.
- [12] Güneyisi E. M. Seismic reliability of steel moment resisting framed buildings retrofitted with buckling-restrained braces. *Earthquake Engineering & Structural Dynamics*, 2012, 41: 853-874.
- [13] Zanini M.A., Hofer, L., Faleschini F., Pellegrino C. The influence of record selection in assessing uncertainty of failure rates. *Ingegneria Sismica*, 2017, 34 (4): 30-40.
- [14] Costanzo S., D'Aniello M., Landolfo R., De Martino A. Critical discussion on seismic design criteria for cross concentrically braced frames. *Ingegneria Sismica*, 2018, 35 (2): 23-36.
- [15] Ferraioli M., Lavino A., Mandara A. Assessment of dynamic increase factors for progressive collapse analysis of steel frames subjected to column failure. *Ingegneria Sismica*, 2018, 35 (2): 67-77.
- [16] Giugliano, M.T., Longo, A., Montuori, R., Piluso, V. Failure mode and drift control of MRF-CBF dual systems. *Open Construction and Building Technology Journal*, 2010, 4: 121-133.
- [17] Longo, A., Montuori, R., Piluso, V. Moment frames – concentrically braced frames dual systems: analysis of different design criteria. *Structure and Infrastructure Engineering*, 2016, 12 (1): 122-141.
- [18] Ohtori Y., Chirstenson R. E., Spencer J. B. F. Benchmark control problems for seismically excited nonlinear buildings. *Journal of Engineering Mechanics*, 2015, 104(4): 366-385.
- [19] SAC Joint Venture. FEMA350 Recommended Seismic Design Criteria for New Steel Moment-Frame Buildings. Federal Emergency Management Agency, USA, June 2000.
- [20] Chen C. C., Chen S. Y. and Liaw J. J. Application of low yield strength steel on controlled plastification ductile concentrically braced frames. *Canadian Journal of Civil Engineering*. 2001, 28(5): 823-836.
- [21] Medina R. A., Krawinkler H. Seismic demands for nondeteriorating frame structures and their dependence on ground motions. Pacific Earthquake Engineering Research Center, 2004.
- [22] Ellingwood B. Mitigating risk from abnormal loads and progressive collapse. *J. Perform. Constr. Facil.* 2006, 20(4): 315-323.
- [23] Li Y., Lu X.Z., Guan H., et al. Probability-based progressive collapse-resistant assessment for reinforced concrete frame structures. *Advances in Structural Engineering*. 2016, 5:1-13.
- [24] Yu X.H., LU D.G., LI B. Estimating uncertainty in limit state capacities for reinforced concrete frame structures through pushover analysis. *Earthquakes and Structures*. 2016, 10(1): 141-161.
- [25] Barbato M., Gu Q. and Conte J. P. Probabilistic Push-Over analysis of structural and soil structure systems. *ASCE Journal of Structural Engineering*. 2010, 136(11): 1330-1341.

- [26] Cornell C. A., et al. The probabilistic basis for the 2000 SAC/FEMA steel moment frame guidelines. *Journal of Structural Engineering (ASCE)*, 2002, 128(4): 526-533.



**ISTRUZIONI PER L'IMPAGINAZIONE DEI LAVORI DA  
SOTTOMETTERE A INGEGNERIA SISMICA**

*Gianmario Benzoni<sup>1</sup>, Fernando Fraternali<sup>2</sup>, Rosario Montuori<sup>2</sup>*

<sup>1</sup>Department of Structural Engineering, University of California San Diego, CA, USA

<sup>2</sup>Dipartimento di Ingegneria Civile, Università di Salerno, Fisciano (SA), Italia

**SUMMARY:** *Il sommario breve in italiano dovrebbe riassumere i contenuti e le conclusioni riportate nell'articolo. Non deve contenere riferimenti bibliografici o equazioni.*

**KEYWORDS:** *keyword 1, keyword 2, keyword 3, keyword 4, keyword 5*

***For not Italian authors this page will be provided by the editors.***